Chemistry Europe
European Chemical Societies Publishing

WILEY VCH

Excellence in Chemistry Research

Announcing our new flagship journal

- Gold Open Access
- Publishing charges waived
- Preprints welcome
- Edited by active scientists

Meet the Editors of *ChemistryEurope*

Luisa De Cola
Università degli Studi di Milano Statale, Italy

Ive Hermans
University of Wisconsin-Madison, USA

Ken Tanaka
Tokyo Institute of Technology, Japan

ChemCatChem

Research Article
doi.org/10.1002/cctc.202300252

Chemistry Europe
European Chemical Societies Publishing

www.chemcatchem.org

Special Collection

Electro-Oxidation of Polyols on Bi-Modified Pt in Acidic Media ($HClO_4$). Understanding Activity and Selectivity Trends

Gabriela Soffiati[+],[a] Victor Y. Yukuhiro[+],[a, b] Swathi P. Raju,[a, b] Matheus B. C. De Souza,[a, b] Leonardo Marquezini,[a, b] Edison Z. da Silva,[c] Pablo S. Fernández,*[a, b] and Miguel A. San-Miguel*[a]

Herein we show that Pt(111) and Pt(100) can produce the ketone through the oxidation of the secondary carbon of the polyols. After the Bi modification, the selectivity for the ketone formation increases. On the other hand, we observe that pure and Bi-modified Pt(110) only produced the C3 molecules oxidized in the primary carbon, and it is the only facet that shows an enhancement in the activity due to the modification. In line with these findings, small Pt nanoparticles are not selective for ketone formation. Finally, based on data obtained through DFT calculations, we suggest that positively charged Bi adatoms interact with the OH- groups of the enediol-like intermediate (believed to be the precursor for the ketone/aldehyde production), facilitating the oxidation of the secondary carbon to produce DHA.

Introduction

The use of biomass-derived energy sources has been on the rise since the mid-1990s, a trend that will persist in the following decades as the world seeks to move from fossil fuel-based energy sources to renewables.[1] These biomass-based energy sources range anywhere between C_1 and C_6 oxygenated compounds, from formic acid[2] to sorbitol[3] and glucose,[1] and some of them, such as glycerol (GlOH),[4] can also be used to synthesize platform chemicals of common industrial interest.[5]

In the context of the energetic transition, the (electro−)oxidation of biomass-derived resources emerge as a great opportunity. By using electrolyzers, it is possible to concomitantly obtain value-added chemicals and high-purity hydrogen in the anode and cathode, respectively.[6–8]

Several catalysts for the (electro−)oxidation of these compounds have been published in the literature, ranging from mono to multi-metallic alloys supported on carbon derivatives or metal oxides[9,10] to nanoparticles with core-shell structures or controlled shapes.[1] Among all these chemicals, the common denominator is the use of noble metals, for instance, Au, Pd, and Pt, which can oxidize all of those biomass-derived oxygenated compounds with various degrees of efficiency.[11] Of particular interest is the modification of platinum by incorporating Bi, as it changes the selectivity of the reaction.[3,8,12–16]

This finding was first reported by Kimura et al.[12] when studying glycerol oxidation after incorporating Bi to Pt-supported on charcoal. On the unmodified Pt catalyst, the main oxidation products are glyceraldehyde and glyceric acid, generated from the oxidation of the primary carbon. After adding Bi, dihydroxyacetone (DHA) was the main oxidation product of the reaction, generated from the oxidation of the secondary carbon. The authors proposed that the Bi adatoms worked as site blockers on the Pt surface, controlling the orientation of glycerol so that the oxidation of the secondary carbon is preferred. This change in selectivity, from the oxidation of primary to secondary carbon, was also observed in other molecules, including aldonic acids,[13,14] fructose,[15] sorbitol,[3] and glucose.[16] Similar results were also observed using Pd instead of Pt[15,16] and with Pb instead of Bi.[13]

In aqueous phase heterogeneous catalysis, this change in selectivity has been rationalized on the basis of a chelate complex formed between the molecule and the promotor,[13,14,16] where 2 or 3 oxygen atoms of the hydroxyl groups of these oxygenated compounds are interacting with the deposited adatom.

This increase in the selectivity for the oxidation of the secondary carbon in the presence of Bi has also been observed in electrochemical ambient; however, the selectivity and conversions are much lower. Kwon et al.[5] reported the same

[a] G. Soffiati,[+] V. Y. Yukuhiro,[+] S. P. Raju, Dr. M. B. C. De Souza, L. Marquezini, Dr. P. S. Fernández, Dr. M. A. San-Miguel
Institute of Chemistry
Department of Physical Chemistry
State University of Campinas
R. Josué de Castro, s/n
13083-970 Campinas (Brazil)
E-mail: pablosf@unicamp.br
smiguel@unicamp.br
[b] V. Y. Yukuhiro,[+] S. P. Raju, Dr. M. B. C. De Souza, L. Marquezini, Dr. P. S. Fernández
Center for Innovation on New Energies (CINE)
R. Michel Debrun, s/n, Prédio Amarelo
13083-841 Campinas (Brazil)
[c] Dr. E. Z. da Silva
Institute of Physics "Gleb Wataghin" (IFGW)
State University of Campinas
R. Sérgio Buarque de Holanda, 777
13083-859 Campinas (Brazil)
[+] These authors contributed equally.

Supporting information for this article is available on the WWW under https://doi.org/10.1002/cctc.202300252

Special Collection *This publication is part of "Catalysis in Latin America". Please check the ChemCatChem homepage for more articles in the collection.*

change in selectivity described in heterogeneous catalysis when using Bi-modified Pt/C nanoparticles for the electro-oxidation of glycerol (EOG) in an acidic solution (H_2SO_4). However, the selectivity depends strongly on the electrochemical potential, and DHA is the main product only in a narrow potential window. Using in situ Fourier-transform infrared spectroscopy (FTIR), the authors showed that the adsorption of Bi blocked the adsorption of CO on platinum, a common poisoning agent in the oxidation of organic molecules. They also investigated the possible complexation between Bi and glycerol, as proposed in the works of Kimura et al.[12] and other authors.[13–16] While no evidence to support a liquid phase complex between Bi and glycerol was found, their results pointed towards the idea of a surface complexation between the adatom and the oxygenated molecule, as seen by the increased Pt activity towards the electro-oxidation of 1,3 propanediol in the presence of Bi. Later, using density functional theory (DFT), Garcia et al.[17] explained the reaction selectivity for the electro-oxidation of glycerol on platinum single crystal electrodes,[18] namely Pt(100) and Pt(111), by looking at the relative stability of adsorbed double-dehydrogenated intermediates (Figure 9). They proposed that Pt(111) produces DHA due to the higher relative stability of the enediol-like intermediate in this surface, formed by the dehydrogenation of the primary and secondary carbons. Unlike the other intermediates, formed by adsorption through either one or both primary carbons, the enediol-like intermediate could isomerize to yield either glyceraldehyde or DHA. On the other hand, this intermediate is not stable enough on Pt(100), where only glyceraldehyde and glyceric acid were observed. A subsequent article by the same group[19] hypothesized that Bi enhances DHA production in Pt(111) by further stabilizing this intermediate.

Finally, we have shown[20] that the trend observed for the oxidation of glycerol on Pt can be extended to polyols with longer chains (Figure 9), suggesting that the oxidation of the secondary carbon depends on the relative stability of enediol-like intermediates. However, despite the chemical consistency of these results, the relatively low energy difference between the intermediates must be noted. It is also important to point out that, according to Garcia et al.[17] and Soffiati et al.,[20] the intermediates are adsorbed on Pt and partially dehydrogenated, in contrast with those proposed by Kimura et al.[12] We believe that the choice of these adsorbed intermediates is reasonable since Pt is a well-known catalyst for the adsorption and dehydrogenation of organic molecules.[21,22] Besides, this phenomenon has been broadly discussed and is well-accepted for other small organic molecules in similar systems to this work.

Despite the studies, there are still several partially or non-answered questions, namely:

1) Are indeed the double-dehydrogenated intermediates able to explain the selectivity trends for polyols in terms of the coordination of the Pt atoms at the catalyst surface?
2) Can we relate activity and selectivity trends to the coordination of the Pt atoms at the catalyst surface in the presence and absence of Bi?
3) Why ~3 nm diameter spherical Pt nanoparticles show high selectivity for DHA, being that it was observed only on Pt(111) single crystals in previous publications?

To help answer these questions, we repeated the experiments by Garcia et al.[17] and Kwon et al.,[5] i.e., we studied the electro-oxidation of glycerol using electrochemical, analytical, and computational techniques on different Pt surfaces. However, in our case, the experiments with glycerol were not only performed with Pt(111) and Pt(100), we also included Pt(110). In this contribution, the use of D_2O in the FTIR experiments is critical as it permits tracking the changes in the production of DHA in the presence and absence of Bi. The use of H_2O strongly distorts the spectra in the region of the most important bands attributed to carbonyl-containing compounds. Besides, we studied the stability of the double-dehydrogenated intermediates of glycerol and erythritol on Pt(111) in the presence and absence of Bi through computational experiments. Finally, to understand the effect of the Bi oxidation state, we modeled the double-dehydrogenated intermediates of glycerol on Pt(111) in the presence of Bi_2O_3 and studied the stability and charge distribution in the system.

Our results show that the oxidation of the secondary carbon of polyols is more likely as the coordination of the Pt atoms at the catalyst surface is higher. In line with this, we show that small Pt nanoparticles do not produce a high selectivity to the ketone. Besides, the computational experiments show relatively low energy differences for the adsorbed double-dehydrogenated intermediates, both in the presence and absence of Bi species. We think these minor energy differences somehow explain the low selectivity of the reaction in almost all the potential windows usually explored in this field. However, a careful analysis of the charge distribution clearly shows a strong interaction between the oxidized Bi atom and the HO-groups of the enediol-like intermediate. We propose here a new idea that helps us explain the increase in the selectivity to the formation of the ketone through differences in the bond strengths of the primary and secondary HO groups of this key adsorbate.

Results and Discussion

Electrochemical results

Figure 1 shows the electrochemical results for the pure and Bi-modified Pt electrodes. The voltammetric profile of the EOG for the electrodes without the Bi-modification is similar to those reported elsewhere.[17,23,24] However, for the Bi-modified electrodes, the voltammetric shape for the Pt(111) and Pt(100) are similar but not equal to some previous reports,[19] i.e., while we had a decrease in activity for both electrodes, the authors observed an increase for Pt(111).

After the Bi-modification of Pt(111), the relatively intense peak at ~0.6 V does not appear. The current that was observed at this potential for the pure Pt(111) is probably mainly due to the CO oxidation (a specie that was previously formed due to the dissociative adsorption[25] of glycerol) to CO_2 through Langmuir-Hinshelwood mechanism. After the Bi-modification,

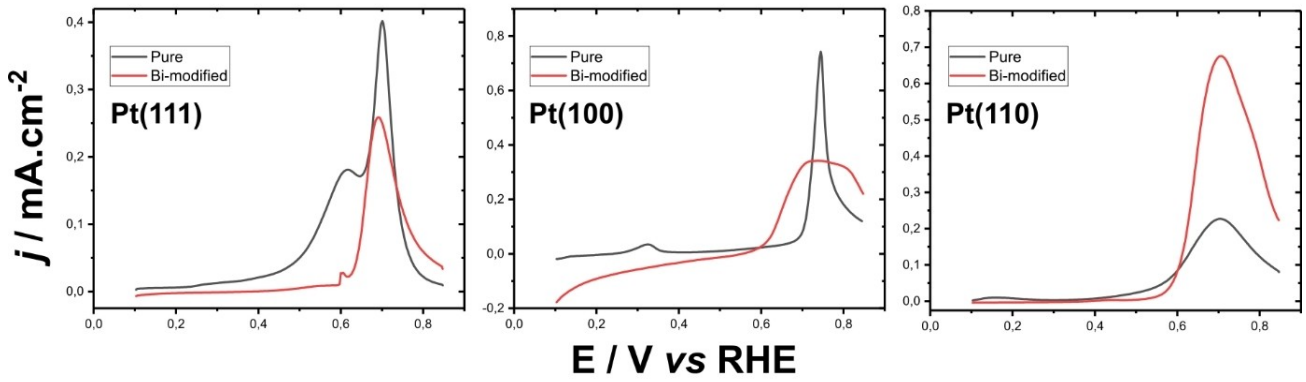

Figure 1. First positive-going scan of the EOG for the different Pt surfaces with/without Bi-modification. All measurements were performed in 0.1 M GlOH + 0.1 M $HClO_4$ at 10 mV s^{-1}.

the current had a drastically decrease because the Bi adatoms on the Pt hinder the CO formation. For the Bi-modified Pt(100), the peak at ~0.3 V (again associated with the dissociative adsorption) does not appear.[25] For Pt(110), we can observe an increase in its activity when Bi modifies the electrode, and we do not observe the weak peak at ~0.15 V that appears for the pure Pt(110). Thus, we conclude that the presence of Bi avoids the dissociative adsorption of the molecule, which is likely a site demanding reaction as was elegantly demonstrated for the CO formation through the adsorption of methanol on Pt(111).[26] Finally, it is important to note that a similar result was found for the same system in alkaline media,[27,28] leading us to the conclusion that the increase in the activity of polycrystalline Pt electrodes (for instance, nanoparticles) is due to the activation of low-coordinated Pt atoms by preventing their poisoning. After obtaining and comparing the voltametric behaviour for the pure[17,23] and Bi-modified Pt,[19] we performed in situ FTIR measurements for each facet.

In situ FTIR results

Figure 2(a,b) shows the spectra obtained for the pure Pt(111) and Bi-modified Pt(111), respectively. For pure Pt(111), a band at 2050 cm^{-1}, related to the formation of linearly-bonded CO to Pt (CO_L), started to appear at 0.4 V. At 2345 cm^{-1} a band related to CO_2 production can be observed. The appearance of this band matches the decrease of the intensity of the CO band, indicating that the CO_2, at least in part, comes from the oxidation of the adsorbed CO, which is a well-stablished result in the literature for this system.[29,30] For the Bi-modified Pt(111), a weak band related to CO_L appeared at 0.6 V and vanished at 0.7 V, explaining the difference in the electrochemical results for these surfaces, i.e., the Bi adatoms decreased the quantity of CO that is formed due to the dissociative adsorption, hence less CO is oxidised to CO_2, lowering the current density. Therefore, CO_2 was not observed for the modified electrode. The inhibition of the CO formation has also been observed for glycerol in alkaline media and other small organic molecules.[27,28,31,32]

The bands at 1735 cm^{-1} and 1435 cm^{-1} are related to the production of carbonyl-containing compounds and ketones, respectively, as seen on the spectra of figure S2.[19,33] For the Pt(111), these bands start to appear at 0.6 V, while for the Bi-modified Pt(111), the band at 1735 cm^{-1} begins at 0.5 V. Besides, there is an increase in the relative intensity of the features at 1735 cm^{-1} and 1435 cm^{-1} at higher potentials in comparison with the pure Pt(111). Therefore, in agreement with the literature,[19] we conclude that the presence of Bi reduces the C–C bond breaking (decreasing the catalyst poisoning from CO), increasing the selectivity towards DHA and other carbonyl-containing compounds.

Figure 2(c,d) shows the results for Pt(100) and Bi-modified Pt(100), respectively. Pure Pt(100) is the only facet that showed a band at 1860 cm^{-1}, related to bridge-bonded CO (CO_B).[17] At 0.4 V, the CO_L band starts to appear and remains until 0.7 V. As the electrochemical potential increases, the CO_L band becomes more intense, and the CO_B feature decreases, showing a conversion between CO_L and CO_B. At 0.7 V, a band at 2345 cm^{-1}, related to the formation of CO_2, appears, and the bands related to CO_L and CO_B start to decrease, showing that part of the CO_2 band is due to the oxidation of CO to CO_2. For the Bi-modified Pt(100), no CO and CO_2 formation was observed during the whole potential range. The bands at 1735 cm^{-1} and 1435 cm^{-1}, related to carbonyl-containing compounds and ketone formation, respectively, start to appear at 0.7 V for the Pt(100). On the other hand, for Bi-modified Pt(100), the bands at 1735 cm^{-1} and 1435 cm^{-1} appear at 0.6 V and 0.7 V, respectively. More importantly, both bands at 1735 cm^{-1} and 1435 cm^{-1} are more intense than for the pure Pt(100) at the same potential, indicating a higher production of carbonyl-containing compounds. Thus, the Bi-modification effect for the Pt(100) was also to avoid CO poisoning (which is more intense than for Pt(111)) and increase the relative intensity of the carbonyl-containing compounds and DHA bands, showing the improvement of the selectivity to these products.

Finally, Figure 2(e,f) shows the results for Pt(110) and Bi-modified Pt(110), respectively. The CO_L band (2050 cm^{-1}) arises at 0.2 V for both pure Pt(110) and Bi-modified Pt(110). At 0.5 V a

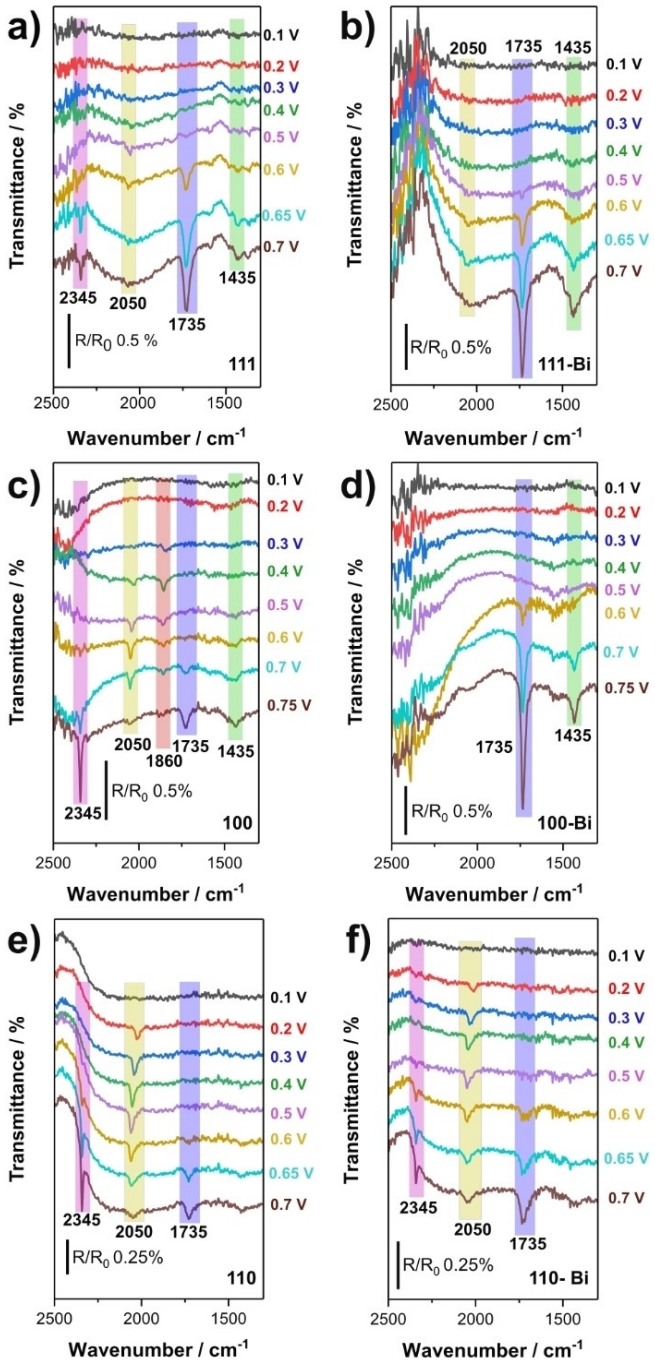

Figure 2. in situ FTIR spectra of: a,b) Pt(111) (left) and Pt(111)/Bi (right); c,d) Pt(100) (left) and Pt(100)/Bi (right); and e,f) Pt(110) (left) and Pt(110)/Bi (right). All measurements were performed in 0.1 M GlOH + 0.1 M $HClO_4$ in D_2O. All spectra are composed of 256 interferograms with 4 cm^{-1} resolution. Reference spectrum acquired at 0.05 V *vs.* RHE.

weak band related to the CO_2 (2345 cm^{-1}) starts to appear for both surfaces. At 0.5 V, the relative intensity of the CO band reaches its maximum to then decrease while the CO_2 band becomes more intense, again suggesting that at least part of CO_2 comes from the oxidation of CO. Bi-modified Pt(110) showed a lower relative intensity of the CO and CO_2 band formation. The carbonyl-containing compound band that appears at 0.6 V for both electrodes has a higher relative intensity for the Bi-modified Pt(110), showing that the Bi-modification may change the reaction pathway to form more carbonyl compounds instead of the full oxidation of the glycerol into CO_2. Besides that, we did not observe the formation of DHA for the pure and the Bi-modified Pt(110). Summarizing, the effect of Bi-modification for Pt(110) was to decrease the relative intensity of the CO and CO_2 bands. Also, the modification increases the intensity of the band related to the carbonyl compounds; however, a significant difference concerning the other facets is the absence of the band at 1435 cm^{-1}, corresponding to the production of DHA.

It is worth mentioning that our measurements are qualitatively similar to those published by Gomes et al.[23] with non-modified electrodes. It is important to remember that, in our case, we used a D_2O instead of H_2O, explaining why our spectra are cleaner in the region between 1400–1800 cm^{-1}, allowing us to draw more conclusions about the development of the bands in this region.

Computational results

Glycerol and Erythritol on Pt(111) Pt(111)/Bi

The double-dehydrogenated derivatives were approximated to the Pt(111) and Pt(111)/Bi surfaces, as described in the experimental section. The adsorption free energy values for glycerol and erythritol derivatives adsorbed on Pt(111) and Pt(111)/Bi are presented in Figure 3.

For the glycerol intermediates (figure 3a), we observe a similar trend of adsorption free energies for both systems, where intermediates 1,3-G and 1,1-G are the most and least stable adsorbed intermediates, respectively. More importantly, by analyzing the changes in the adsorption energy of intermediates with the addition of Bi, we find that 1,1-G and 1,3-G intermediates remain almost with the same energy (destabilization by 0.01 and 0.04 eV, respectively). In contrast, the 1,2-G intermediate, where two neighboring carbons are bonded to the platinum surface (enediol-like intermediate), is stabilized by 0.1 eV.

Figure 3 also shows a similar trend of adsorption free energies between the two surfaces for the erythritol intermediates. The presence of bismuth on the surface does not significantly affects the energy values. The most crucial change was observed for 2,3-E intermediate, one of the possible enediol-like intermediates formed by the adsorption of neighboring carbons and stabilized by 0.1 eV. It is important to note that despite the relatively small energy changes for the systems with and without the adatom, the most stabilized structures were both enediol-type intermediates, indicating some chemical consistency in these results.

Finally, figure 4 shows the structure of the most favorable systems. As discussed before, the presence of Bi stabilizes more the intermediate 1,2-G for glycerol and 2,3-E for erythritol, i.e., the enediol-like intermediates. Another important point is that our results show that the Bi adatoms present a positive net

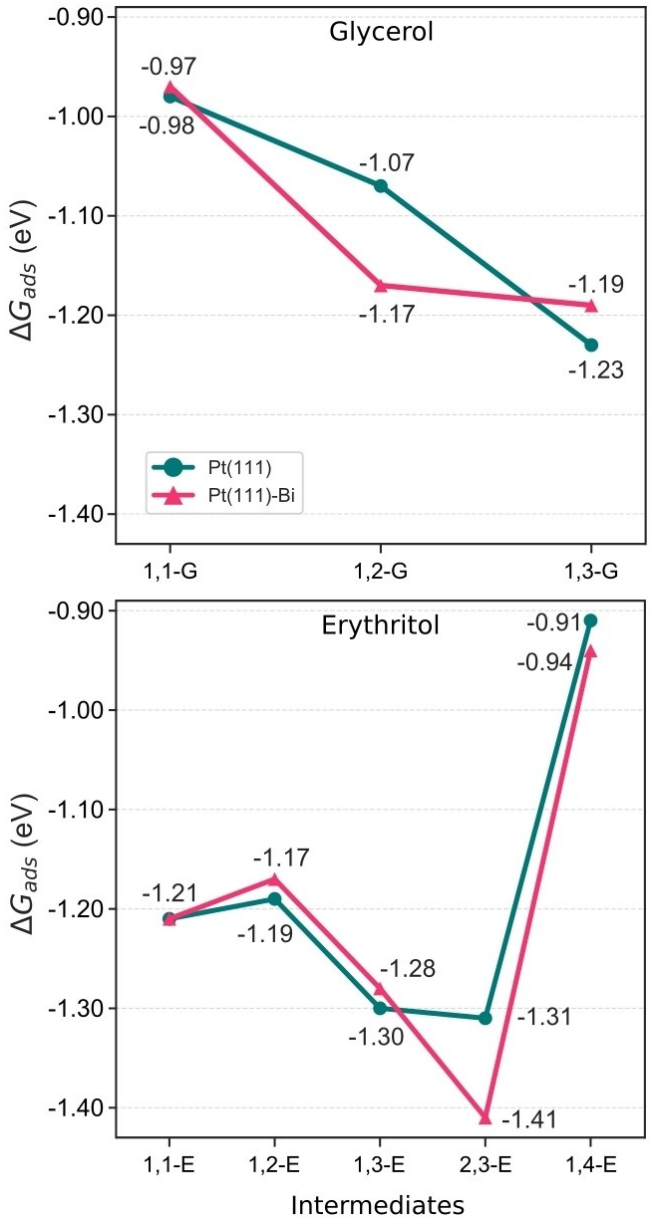

Figure 3. Adsorption free energies trends for glycerol and erythritol intermediates. All the intermediates, except for the 1,2-G and 2,3-E (both enediol-like), are equally or less stable in the presence of Bi.

charge (see supporting information for details) and stabilize the intermediates by chelate-like interactions, in which the oxygen atoms from some hydroxyl groups are oriented towards the Bi. We show below that these interactions are essential to understand the selectivity of the oxidation of the primary or secondary carbon of the enediol-like intermediates.

Glycerol on Pt(111), Pt(111)/Bi and Pt(111)/Bi_2O_3

It is well-known that in the electrochemical potential domain explored in this work (0.1-0.85 V), the Bi adatoms change their formal oxidation state from 0 to +3.[34] Thus, to understand the implications of this change in the oxidation state of the adatom, we studied the adsorption of glycerol on *Pt(111), Pt(111)/Bi, and Pt(111)/Bi_2O_3*.

Figure 5 shows the adsorption energies of the double-dehydrogenated intermediates of the electro-oxidation of glycerol. The results showed some differences with respect to the previously reported findings,[20] i.e., we observed in this case, a stabilization of all the intermediates; however, the trends discussed before remain the same.

The keto-enol tautomerism and the related equilibrium between aldoses and ketoses are well-known phenomena in the organic chemistry of carbohydrates.[35,36] Figure 6A shows the multiple steps of the equilibria between the DHA, glyceraldehyde, and the corresponding enolates in alkaline media (it also happens in acid media, but the process is much slower due to difficulty to withdrawing the alpha hydrogen, i.e., the hydrogen atom extracted from the C–H bond). Figure 6B shows the electron and atom re-arrangements necessary for the enediol-like intermediate to be converted either in DHA or glyceraldehyde.

Based on the mechanism proposed above, it is clear the importance of studying the effect of both Bi and Bi_2O_3 adsorption on the charge distribution and bond strengths/distances of the adsorbate. Therefore, we examined the charge distribution on the different systems (figure S5). It is observed that when the adsorbate is on the clean Pt surface, there is a net negative charge flowing from the molecule to the Pt surface. In the presence of Bi, this charge flow decreases, and, very interestingly, in the presence of Bi_2O_3, there is an inversion in the charge flow (see more details in the SI section). Despite the importance of this result, we have still looked at the general parameters of the systems. More specifically, we calculated the charge distribution in all the atoms for all the systems (see SI section). To look at quantities more directly related to our selectivity study, in figure 7, we show how the bond force constant (which is directly related to the bond strength) of the two primary and secondary HO- groups are affected by the presence of Bi and Bi_2O_3.

For the 1,3-G intermediate, we did not observe important changes for any of the HO- groups in the presence and absence of Bi species. On the other hand, 1,1-G and 1,2-G intermediates are more clearly affected by the composition of the surface. For the case of 1,1-G intermediate, results in figure 8 show that in the presence or absence of Bi species, one of the primaries OH-groups (that further from the Bi species) has the weaker H–O bond, which might facilitate the formation of the aldehyde (figure 6). In the case of 1,2-G, the H–O bond strength is less sensitive to the presence of Bi species; however, remarkably, the weakest H–O bond belongs to the group attached to the secondary carbon when it directly interacts with Bi_2O_3, favouring the formation of DHA.

In this work, we used electrochemical, spectroscopic, and computational methods to shed light on general trends for the electro-oxidation of polyols on Pt surfaces, both in the presence and absence of Bi adatoms in acidic media.

First, the electrochemical experiments led us to the same conclusion that was reached in alkaline media for our group,

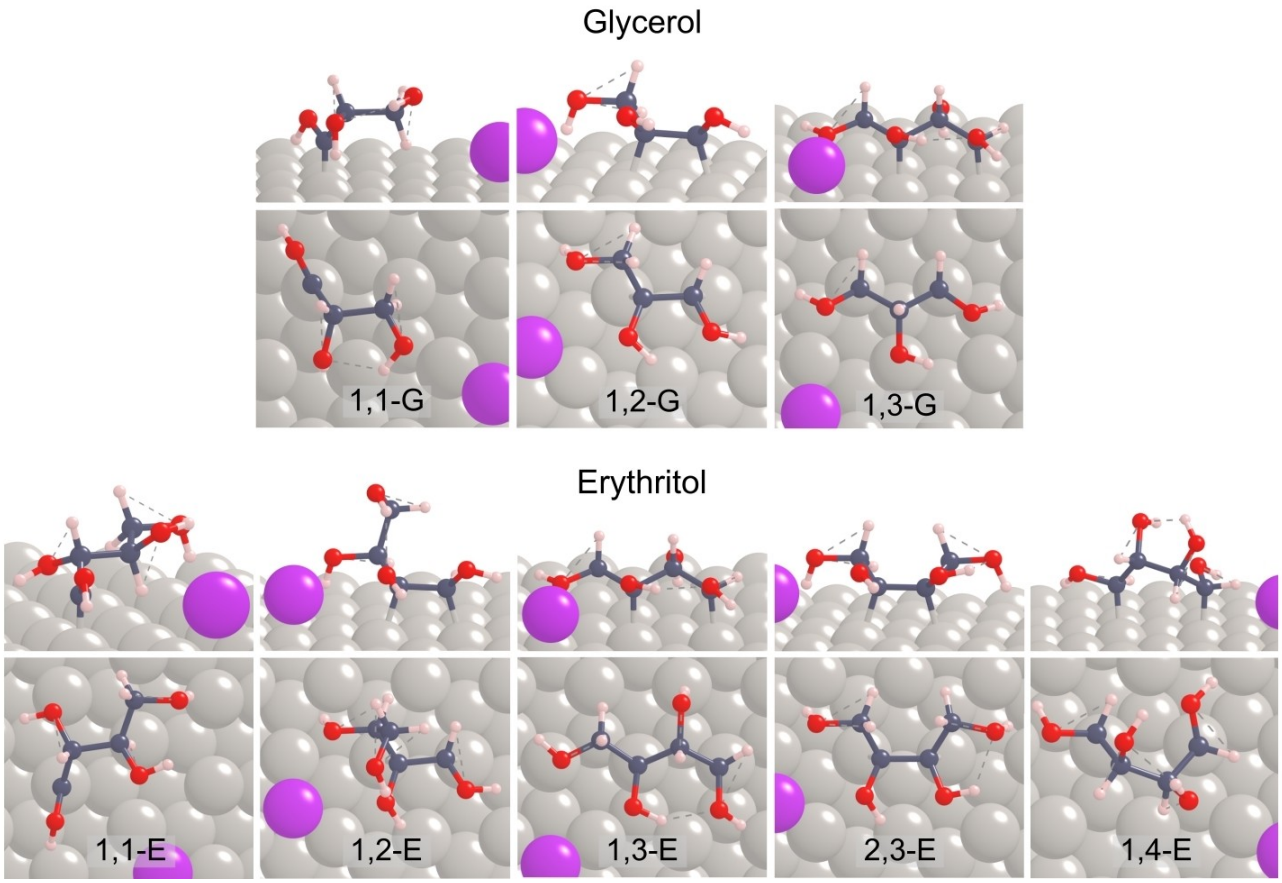

Figure 4. Top and side views of glycerol and erythritol intermediates on Pt(111)/Bi surface. The numbers indicate the carbons of glycerol (G) and Erythritol (E) bound to the surface.

i.e., the adatoms act by mainly activating the electro-oxidation of glycerol on low-coordinated Pt atoms.[27,28]

The in situ FTIR results are in line with the literature[17,23] in the sense that it is well-known that both Pt(100) and Pt(110) form much more CO than Pt(111) and that the introduction of Bi decreases the poisoning by CO as was previously observed for glycerol[19,27,28] and other small organic molecules.[31,32] On the other hand, we show here for the first time this trend for Pt(111), Pt(100), and Pt(110) in the presence and absence of Bi.

However, the most crucial point of the contribution of the FTIR is that by avoiding the use of regular water, we were able to follow through with this extremely sensitive technique the formation of DHA, something that is tricky to be done with other methods (except for experiments involving high glycerol conversion, such as long-term electrolysis). Thus, we show here that both Pt(111) and Pt(100) surfaces can form DHA and that the selectivity for the generation of this product increases when Bi modify these surfaces. On the other hand, Pt(110) is not able to appreciably oxidize the secondary carbon of polyols either before or after the modification by Bi.

To test the general validity of our observations by applying model surfaces, we performed in situ FTIR using small spherical nanoparticles (see details in the supporting information section). Figure 8 shows the results obtained before and after the modification by Bi. The comparison of figure 8A and 8B with figure 2 shows that the NPs behave more similarly to Pt(110), i.e., the spectra do not show the presence of DHA in the unmodified and modified electrode. The result is reasonable as this material does not contain well-ordered facets; however, it is worth noticing that there are contributions in the literature showing outstanding selectivity results to DHA in H_2SO_4 solutions.[5] To check if the differences are due to an effect of the anion adsorption, we repeated the experiment in H_2SO_4 solution, but we observed slight differences (figure S3). Besides, it is well known that by increasing the glycerol concentration, the selectivity to products without C–C bond breaking increases.[25] Gomes et al. claimed that there is a partial inhibition of CO_2 formation, mainly at lower potentials (below 0.7 V *vs* RHE) because the high glycerol concentrations displace the hydroxyl species from the Pt surface, partially inhibiting the CO_2 formation. Among other findings, the authors demonstrated that the CO coverage increases with the glycerol concentration. We believe that this strong adsorbate can act in a similar way to Bi, i.e., its presence decreases the probability of the adsorption through multiple carbons, reducing the C–C bond breaking.

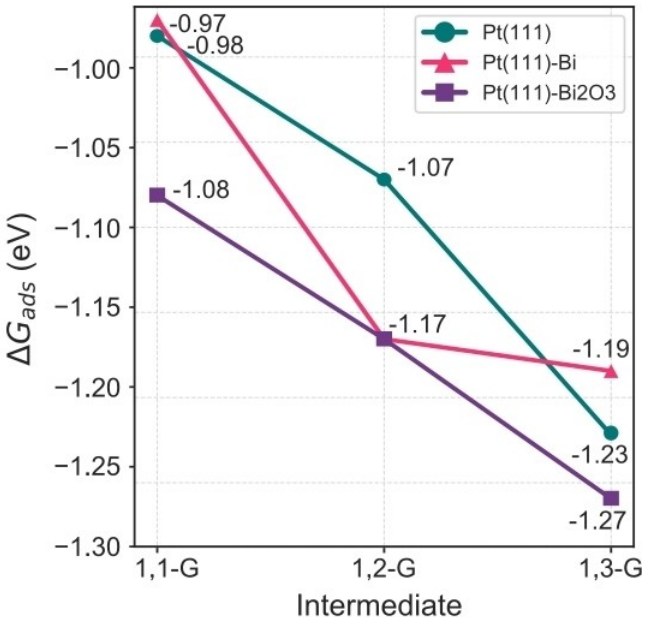

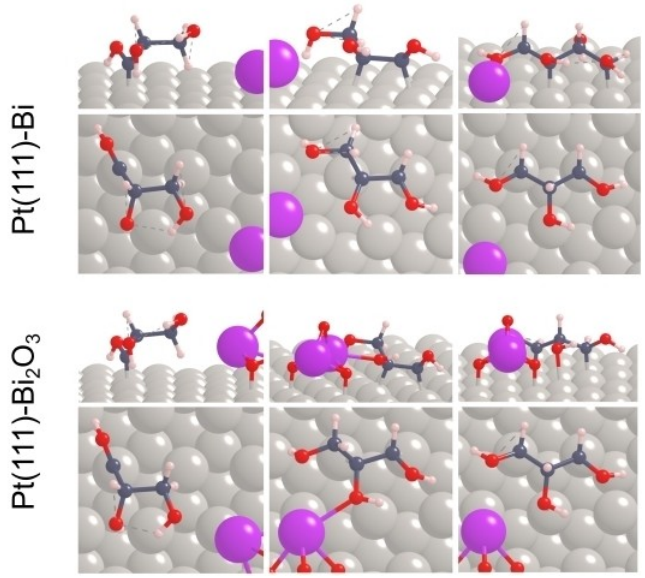

Figure 5. Adsorption free energies for the glycerol intermediates on the three different Pt surfaces. The structures for Pt(111)-Bi and Pt(111)-Bi_2O_3 models are also presented.

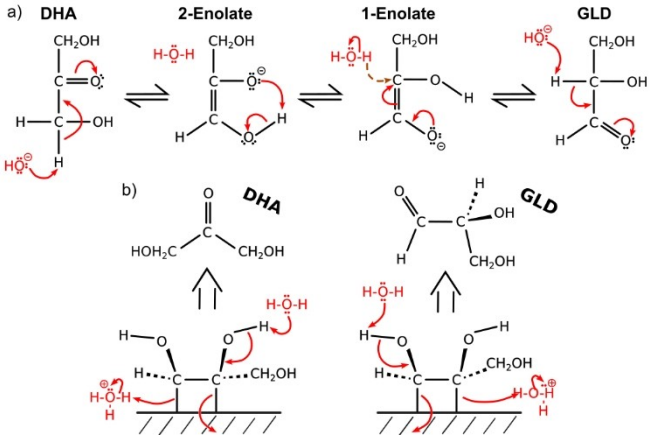

Figure 6. (a) Multiple equilibria between DHA, the primary and secondary enolates, and GLD (keto-enol tautomerism). (b) Proposed atom and electron re-arrangements to convert the enediol-like intermediate of glycerol to DHA or GLD.

Therefore, we repeated the experiment of figures 8A–B but changing the glycerol concentration from 0.1 to 1 M. Results show again that the selectivity to DHA is much smaller than in Pt(111) and Pt(100), but that the Bi adatoms also promote the production of DHA on these relatively small nanoparticles, partially justifying previous results from the literature.

To deepen our understanding of the selectivity results described in this article, we studied the stability of double-dehydrogenated polyol adsorbates on Pt(111), Pt(111)/Bi, and Pt(111)/Bi_2O_3. These intermediates have provided some insight into understanding the trends shown for the products (without C–C bond breaking) of the oxidation of the polyols on Pt(111), Pt(100), and Pt(110).[17,20] Here, we used the same intermediates to understand the trend in the oxidation of polyols on Pt surfaces in the presence of Bi, i.e., the enhancement in the oxidation of the secondary carbon to produce the corresponding ketone.

Our hypothesis was that if the model involving the double-dehydrogenated intermediates is correct, and if the enediol-like intermediates are the precursors of the ketones, then the addition of Bi in the systems should stabilize these intermediates more than the others. Despite the relatively small energy differences, we indeed found this result for glycerol and erythritol.

In this work, we have carefully looked at the required electrons and atoms re-arrangements for transforming the enediol-like intermediate in the aldehyde or the ketone (figure 6). Differently to the corresponding equilibria in solution, as the Pt-based surface has catalyzed the de-hydrogenation process to form the intermediates, the next step to form the aldehydes or the ketone is a chemical reaction that consists of electrons rearrangements and an OH bond breaking. Our calculations show that the presence of oxidized Bi atoms (Bi_2O_3) weaken preferentially the secondary OH bonds resulting eventually in a lower activation energy to produce the DHA (see figure 6) and explaining the observed promotion of the DHA formation.

The mechanisms of the electrooxidation of polyols contain several parallel steps, including many transfers of electrons and protons.[37–39] The study of the relatively simple pathways to form products without C–C bond breaking, which generally leads to the most valuable chemicals, is rather complicated. As shown here, several double-hydrogenated adsorbates can be possible and adopt several configurations with different energies. In our work, the problem is even more complex as the presence of Bi adds several degrees of freedom when considering various adsorption sites, interactions with other species, and even different possible oxidation states. Glycerol has been the most studied polyol, and an excellent review by Li

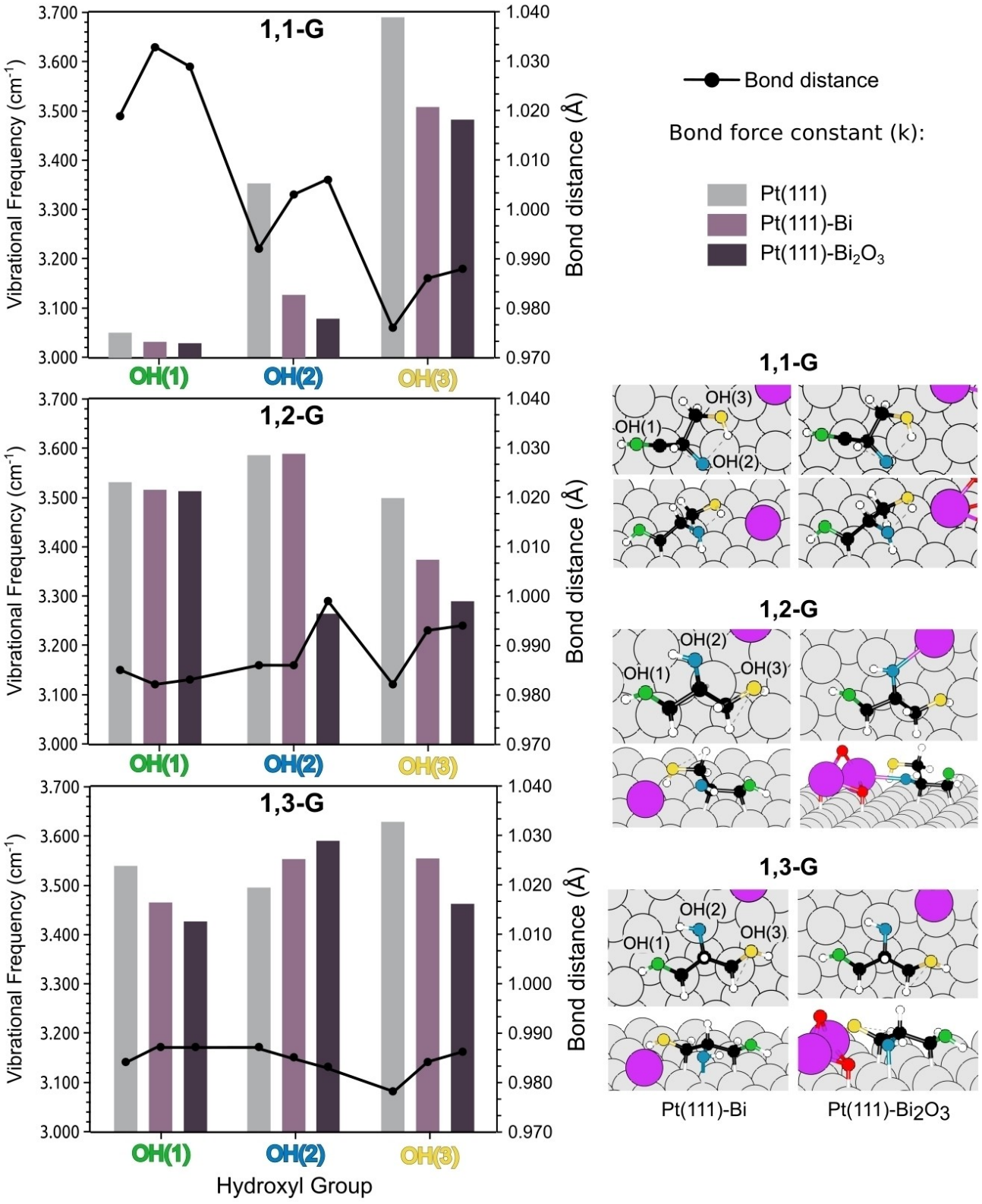

Figure 7. Vibrational frequencies, represented by the columns, and bond distances, represented by the black curves, for the O–H bonds of the glycerol intermediates. The three different hydroxyl groups for each intermediate are represented by green, blue, and yellow colors and can be identified in the structures presented on the right panel. The results are shown for all explored surfaces.

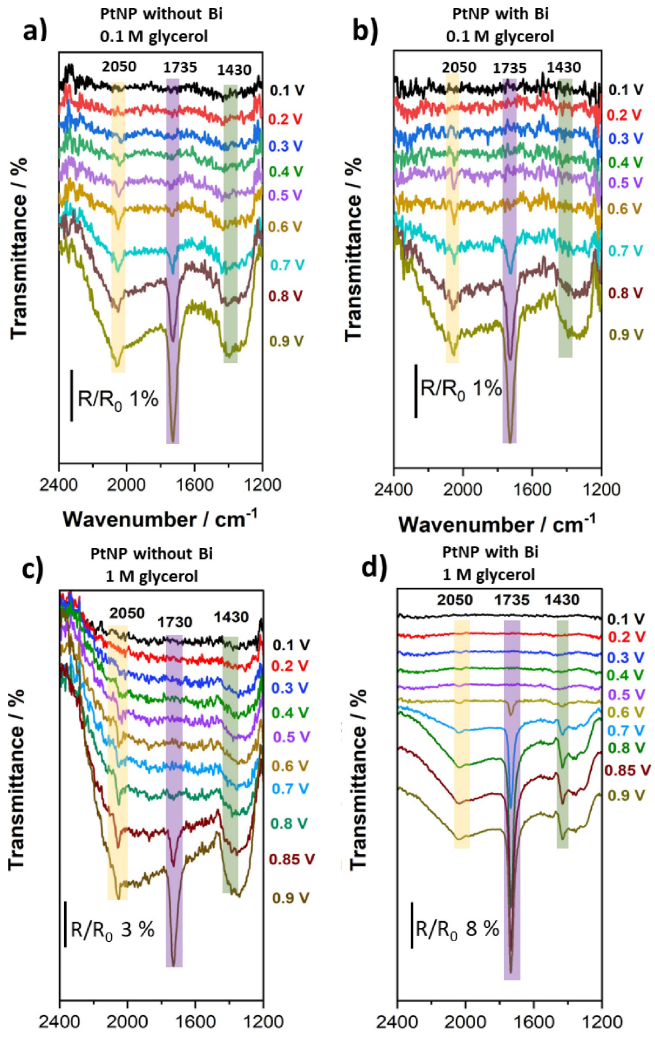

Figure 8. in situ FTIR spectra of Pt NPs (A and C) and Bi-modified Pt NPs (B and D) in X M GlOH + 0.1 M $HClO_4$ in D_2O. Spectra A and B were obtained for X = 0.1 M, and C and D for X = 1 M. All spectra are composed of 256 interferograms with 4 cm^{-1} resolution. Reference spectrum acquired at 0.05 V *vs.* RHE.

and Harrington shows this complexity.[37] Despite the several works published in this field, this study brings a new and simple idea to the discussion of the selectivity of this reaction for the formation of C3 products, paving the way for further studies involving others adatoms and surfaces. Thus, we hypothesize that a similar effect could be observed with a different positively charged adatom than Bi.

Conclusion

In this work, we showed that both Pt(111) and Pt(100) could oxidize the secondary carbon of the polyols. On the other hand, the corresponding ketone was not observed on Pt(110). Besides, we showed that the presence of Bi does not increase the activity of Pt(111) and Pt(100) but enhances the selectivity for the formation of the ketone. On the other hand, Pt(110) is activated by Bi, but it continues without being able to oxidize the secondary carbon of polyols. Consistently with these results, the oxidation of glycerol on small Pt nanoparticles in the presence of Bi does not promote the oxidation of the secondary carbon in the same experimental conditions.

The study of the stability of the double dehydrogenated derivatives of glycerol and erythritol suggests that the presence of Bi adatoms on Pt(111) increases the energy of all the intermediates, except for those adsorbed through neighboring carbon atoms (enediol-like intermediates), which are believed to be the precursors for the oxidation of secondary carbons of polyols. We also report that oxidized Bi species interact with the enediol-like intermediate in such a way that facilitates the conversion of this intermediate in a ketone better than in the corresponding aldehyde.

Experimental Section

Electrodes preparation and electrochemical experiments

All measurements were performed at room temperature in a clean standard three-electrodes cell controlled by a PGSTAT 204 potentiostat from Autolab®. We used a 0.28 cm^2 Pt single-crystal disk with (111), (100), and (110) facets as Working Electrode (WE). The electrodes were purchased from Mateck®, polished on the oriented side with roughness <0.01 micron and orientation accuracy <0.1 degrees. Prior to each experiment, the surface was cleaned by forming a meniscus with an aqua regia solution for 5 s (to eliminate the Bi), followed by rinsing with ultrapure water (this procedure was repeated once). Afterward, the electrode was flame annealed in a butane-oxygen flame for approximately 1 minute, followed by cooling in a reductive atmosphere composed of Ar/H_2 (~2:1) for ~75 s. The surface was then protected by a droplet of ultrapure water saturated with Ar/H_2 to prevent contamination and surface disordering during the transfer to the electrochemical cell. Besides, we used a spiral Pt wire as a Counter Electrode (CE) and a Reversible Hydrogen Electrode (RHE) as Reference Electrode (RE) in all measurements. Blank voltammograms were acquired in O_2 free 0.1 M $HClO_4$ for each facet before the electrochemical experiment to check the system cleanliness and surface orientation. The blank voltammograms were recorded in a range of 0.05 V to 0.9 V for Pt(111) and 0.05 V to 0.8 V for Pt(100) and Pt(110) at 50 $mV\,s^{-1}$. For the experiments without the adatoms, the electrodes were protected with an electrolyte drop and transferred to another electrochemical cell containing 0.1 M GlOH + 0.1 M $HClO_4$ after acquiring the blank. For the Bi-modified electrodes, a Bi adlayer was prepared by irreversible adsorption, which consists of putting the electrode in contact with a Bi_2O_3 solution (~10^{-4} M) for ~20 s, after which the electrode surface is completely saturated with a Bi adlayer, i.e., all surface Pt atoms are unavailable for hydrogen adsorption/desorption.[34] The Bi coverage on the Pt/Bi electrodes depends on the time of contact and the Bi concentration. Using the conditions mentioned above, and with small (<0.5 cm^2) Pt single crystals, a ~20 s contact time was sufficient to cover their surface fully. Then, the electrode is transferred to the electrochemical cell containing 0.1 M GlOH + 0.1 M $HClO_4$. For the EOG experiments, the voltammogram was recorded in a range of 0.1 V to 0.85 V at 10 $mV\,s^{-1}$.

In situ FTIR experiments

All in situ FTIR experiments were performed in a Shimadzu IR Prestige-21 spectrometer with mercury cadmium telluride (MCT) detector. A spectroelectrochemical cell equipped with CaF_2 prism was used on top of a specular reflection accessory (VeeMax II, Pike Technologies). All spectra in this work are represented in transmittance (%).

For the spectroelectrochemical measurements, the Pt Single-Crystal electrodes were prepared in the same way as for the electrochemical results. In the case of the spherical nanoparticles (See Supporting Information), we deposited 50 μL of the nanoparticle ink on the gold (Ø = 7 mm) surface. Besides, we used a Pt foil as CE and RHE as RE in all experiments.

After preparing the electrode, it is polarized at 0.05 V and then inserted in the spectroelectrochemical cell, in contact with the electrolyte, and pressed onto the prism to form a thin layer. In this experiment, the spectra were obtained during a stepped chronoamperometry in a range of 0.10 V–0.70 V for Pt(111) and Pt(110), 0.10 V–0.75 V for Pt(100), and 0.10 V–0.9 V for the spherical (polyoriented) nanoparticles. 256 interferograms with a resolution of 4 cm^{-1} were acquired at each potential. The same set of experiments was repeated in 0.5 M H_2SO_4 using Pt spherical nanoparticles in 0.1 M and 1.0 M glycerol concentrations. The spectra were plotted as the ratio R/R_0, where R_0 is the reference spectrum collected at 0.05 V and R is the sample spectra in function of potential. All measurements were performed in D_2O, and all potentials were applied *vs.* RHE. The use of D_2O instead of H_2O is critical for this investigation, as regular water has a higher IR absorption than D_2O. Thus, the bands due to the carbonyl groups are much easier to be followed in the results shown here than in others obtained in similar systems in the literature. In particular, the band due to the formation of DHA around 1435 cm^{-1} can be ideally detected and followed in our spectra, something that is not straightforward by using other commonly used techniques in the field, like HPLC.

Chemicals

The solutions for the electrochemical experiments were made with ultrapure water (18.2 MΩ cm, 25°C, Millipore) and for the in situ FTIR experiments, solutions were prepared by using deuterium oxide (99.9% atom% D, Sigma-Aldrich). All chemicals were used without prior purification. The chemicals employed were perchloric acid (70% ISO grade, Merck Emsure®), sulphuric acid (95-97%, ISO grade, Merck Emsure®), Bismuth (III) oxide (ReagentPlus, Sigma-Aldrich) and glycerol (ACS grade, Sigma-Aldrich).

Computational Methods

The work focuses on the key intermediates of glycerol and erythritol during the oxidation process (Figure 9). DFT-based calculations were carried out with the VASP 5.4 software using Perdew-Burke-Ernzerhof (PBE)[40,41] generalized gradient approximation (GGA) for exchange-correlation functional and Grimme-D3 corrections to account the dispersion effects[42,43] (full details are given in the Supporting Information). Briefly, the simulations were

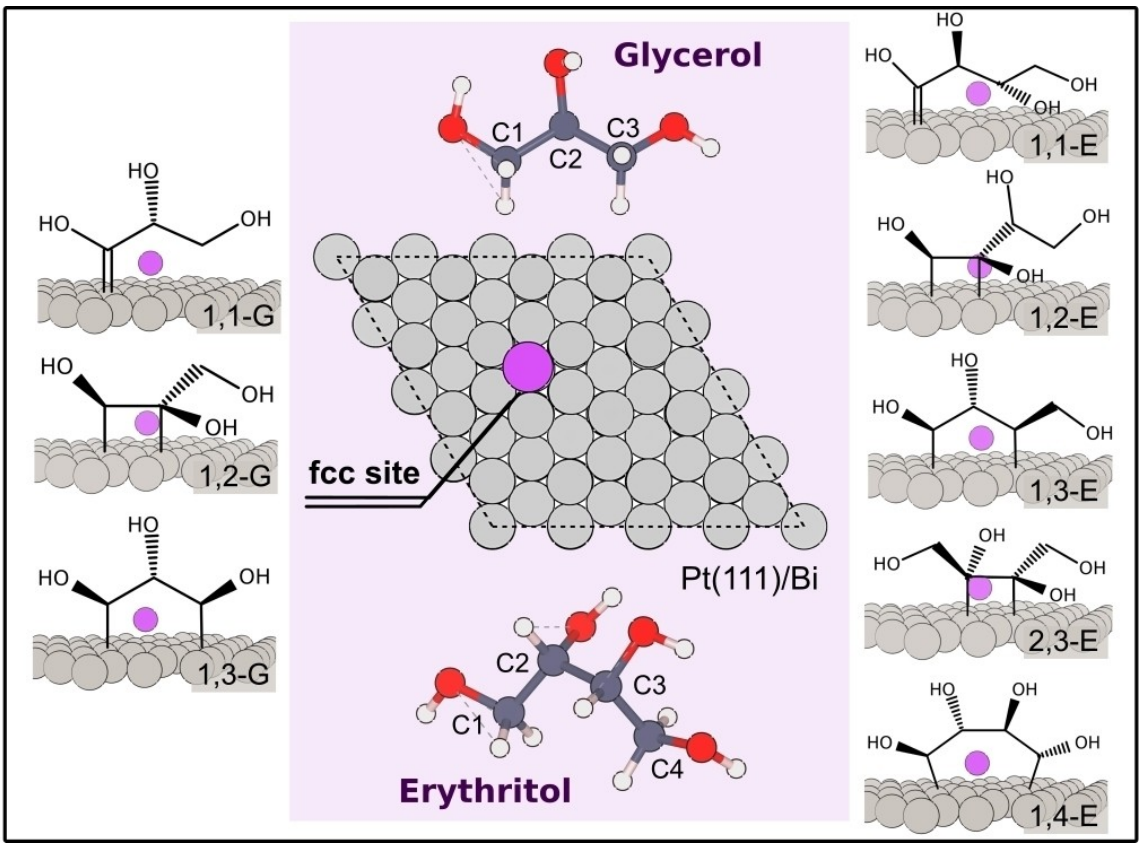

Figure 9. Structure representation of the polyol intermediates explored in this work. Glycerol intermediates on the left side, and erythritol intermediates on the right side. In the middle, the surface and the free molecule structures are shown. The nomenclature follows which carbons are dehydrogenated and bonded to the surface.

carried out using periodic models of adsorption systems composed of three Pt surfaces, Pt(111), Pt(111)-Bi, and Pt(111)-Bi_2O_3, and different adsorbing polyol derivatives. A p(4x4) slab model with five platinum layers and 20 Å of vacuum was chosen to represent the Pt(111) surface. The adsorption of a single Bi atom was found to be more favorable on the fcc site ($\Theta = 1/16$ ML), in agreement with previous reports, and was chosen for the subsequent deposition of the polyol intermediates. The Pt(111)-Bi_2O_3 model followed the structure proposed in Feng et al.,[44] where both bismuth atoms were placed on adjacent sites (one of them fcc, the other hcp) while the three oxygen atoms were arranged between them (Figure S4).

The adsorption free energies provide meaningful thermodynamic information, allowing feasible trends in the stability of the intermediates, which becomes a key factor in understanding surface selectivity. The formation reaction of the intermediates can be represented as:

$$C_nH_{2n+2}O_n + \rightarrow C_nH_{2n}O_n + H_2$$

Where $C_nH_{2n+2}O_n$ is the molecular formula of the polyol, and $C_nH_{2n}O_n$ represents the radical intermediate.

The adsorption free energies can be estimated according to the following equation:

$$\Delta E_{ads} = E_{C_nH_{2n}O_n}* - E - ECnH2n + 2On - EH2 \quad (1)$$

Where $E_{C_nH_{2n}O_n}*$ is the adsorption energy of the adsorbate on the surface, E is the energy for the surface, and the others two terms are related to the free molecules.

$$\Delta G_{ads} = \Delta E_{ads} + \Delta ZPE_{ads} + \Delta U_{ads} + \gamma RT - T \times \Delta S_{ads} \quad (2)$$

The adsorption free energy (Equation 2) is a function of the DFT energy (E), the Zero-Point Energies (ZPE) correction, the thermal contributions[47], the temperature (T) and the entropy (S),[45] where the entropy is equal to a summation over translational, rotational, and vibrational contributions of all reaction components.[46] The corrections are associated with the different scenarios when the molecule is adsorbed or free. Details about these calculations are presented in the Supporting Information.

Acknowledgements

This work was funded in part by "Fundação de Amparo à Pesquisa do Estado de São Paulo – FAPESP" (2013/07296-2, 2016/23891-6, 2016/01365-0, 2017/26105-4, 2017/11986-5, 2019/20874-1, 2020/04431-0); Shell and the strategic importance of the support given by ANP (Brazil's National Oil, Natural Gas and Biofuels Agency) through the R&D levy regulation; "National Council for Scientific and Technological Development – CNPq" [142453/2018-8 and 130741/2021-3] and the Coordenação de Aperfeiçoamento de Pessoal de Nível Superior - Brasil (CAPES) - Finance Code 001. The calculations were performed in the CENAPAD - "Centro Nacional de Processamento de Alto Desempenho em São Paulo", SDumont - "Sistema de Computação Santos Dumont" and CCJDR-Unicamp - "Centro de Computação John David Rogers". The authors also acknowledge the National Laboratory for Scientific Computing (LNCC/MCTI, Brazil) for providing HPC resources of the SDumont supercomputer.

Conflict of InterestData Availability Statement

The authors declare no conflict of interest.

The data that support the findings of this study are available from the corresponding author upon reasonable request.

Keywords: Polyols · DFT · Platinum · Electrocatalysis · Reaction mechanism

[1] Y. Holade, N. Tuleushova, S. Tingry, K. Servat, T. W. Napporn, H. Guesmi, D. Cornu, K. B. Kokoh, *Catal. Sci. Technol.* **2020**, *10*, 3071–3112.
[2] J. V. Perales-Rondón, A. Ferre-Vilaplana, J. M. Feliu, E. Herrero, *J. Am. Chem. Soc.* **2014**, *136*, 13110–13113.
[3] Y. Kwon, E. De Jong, J. K. Van Der Waal, M. T. M. Koper, *ChemSusChem* **2015**, *8*, 970–973.
[4] G. Dodekatos, S. Schünemann, H. Tüysüz, *ACS Catal.* **2018**, *8*, 6301–6333.
[5] Y. Kwon, Y. Birdja, I. Spanos, P. Rodriguez, M. T. M. M. Koper, *ACS Catal.* **2012**, *2*, 759–764.
[6] C. Coutanceau, S. Baranton, *Electrochemical Conversion of Alcohols for Hydrogen Production: A Short Overview*, **2016**.
[7] H. Luo, J. Barrio, N. Sunny, A. Li, L. Steier, N. Shah, I.E. L. Stephens, M. M. Titirici, *Adv. Energy Mater.* **2021**, *11*, 2101180.
[8] J. B. Costa Santos, C. Vieira, R. Crisafulli, J. J. Linares, *Int. J. Hydrogen Energy* **2020**, *45*, 25658–25671.
[9] L. Osmieri, L. Pezzolato, S. Specchia, *Curr. Opin. Electrochem.* **2018**, *9*, 240–256.
[10] C. Coutanceau, S. Baranton, R. S. B. Kouamé, *Front. Chem.* **2019**, *7*, 1–15.
[11] X. Li, L. Zhang, S. Wang, Y. Wu, *Front. Chem.* **2020**, *7*, 1–21.
[12] H. Kimura, *Appl. Catal. A* **1993**, *105*, 147–158.
[13] A. Abbadi, H. van Bekkum, *Appl. Catal. A* **1995**, *124*, 409–417.
[14] P. Gallezot, *Catal. Today* **1997**, *37*, 405–418.
[15] A. W. Heinen, J. A. Peters, H. Van Bekkum, *Carbohydr. Res.* **1997**, *304*, 155–164.
[16] M. Wenkin, P. Ruiz, B. Delmon, M. Devillers, *J. Mol. Catal. A* **2002**, *180*, 141–159.
[17] A. C. Garcia, M. J. Kolb, C. Van Nierop, Y Sanchez, J. Vos, Y. Y. Birdja, Y. Kwon, G. Tremiliosi-Filho, M. T. M. M. Koper, *ACS Catal.* **2016**, *6*, 4491–4500.
[18] V. P. Santos, G. A. Camara, *Results in Surfaces and Interfaces* **2021**, *3*, 100006.
[19] A. C. Garcia, Y. Y. Birdja, G. Tremiliosi-Filho, M. T. M. Koper, *J. Catal.* **2017**, *346*, 117–124.
[20] G. Soffiati, J. L. Bott-Neto, V. Y. Yukuhiro, C. T. G. V. M. T. G. V. M. T. Pires, C. C. Lima, C. R. Zanata, Y. Y. Birdja, M. T. M. M. Koper, M. A. San-Miguel, P. S. Fernández, *J. Phys. Chem. C* **2020**, *124*, 14745–14751.
[21] L. Pérez-Martínez, L. M. Machado de los Toyos, J. J. T. Shibuya, A. Cuesta, *ACS Catal.* **2021**, *11*, 13483–13495.
[22] A. Betts, V. Briega-Martos, A. Cuesta, E. Herrero, *ACS Catal.* **2020**, *10*, 8120–8130.
[23] J. F. Gomes, F. B. C. De Paula, L. H. S. Gasparotto, G. Tremiliosi-Filho, *Electrochim. Acta* **2012**, *76*, 88–93.
[24] T. J. P. Hersbach, C. Ye, A. C. Garcia, M. T. M. Koper, *ACS Catal.* **2020**, *10*, 15104–15113.
[25] J. F. Gomes, C. A. Martins, M. J. Giz, G. Tremiliosi-Filho, G. A. Camara, *J. Catal.* **2013**, *301*, 154–161.
[26] A. Cuesta, *J. Am. Chem. Soc.* **2006**, *128*, 13332–13333.
[27] M. B. C. De Souza, R. A. Vicente, V. Y. Yukuhiro, C. T. G. Pires, W. Cheuquepán, J. L. Bott-Neto, J. Solla-Gullón, P. S. Fernández, *ACS Catal.* **2019**, *9*, 5104–5110.

[28] M. B. C. De Souza, V. Y. Yukuhiro, R. A. Vicente, C. T. G. Vilela Menegaz Teixeira Pires, J. L. Bott-Neto, P. S. Fernández, *ACS Catal.* **2020**, *10*, 2131–2137.
[29] P. S. Fernández, M. E. Martins, C. A. Martins, G. A. Camara, *Electrochem. Commun.* **2012**, *15*, 14–17.
[30] P. S. Fernández, C. A. Martins, M. E. Martins, G. A. Camara, *Electrochim. Acta* **2013**, *112*, 686–691.
[31] S.-C. Chang, Y. Ho, M. J. Weaver, *Surf. Sci.* **1992**, *265*, 81–94.
[32] M. C. Figueiredo, A. Santasalo-Aarnio, F. J. Vidal-Iglesias, J. Solla-Gullón, J. M. Feliu, K. Kontturi, T. Kallio, *Appl. Catal. B* **2013**, *140–141*, 378–385.
[33] P. S. Fernández, P. Tereshchuk, C. A. Angelucci, J. F. Gomes, A. C. Garcia, C. A. Martins, G. A. Camara, M. E. Martins, J. L. F. F. Da Silva, G. Tremiliosi-Filho, *Phys. Chem. Chem. Phys.* **2016**, *18*, 25582–25591.
[34] J. Clavilier, J. M. Feliu, A. Aldaz, *J. Electroanal. Chem. Interfacial Electrochem.* **1988**, *243*, 419–433.
[35] I. Delidovich, R. Palkovits, *ChemSusChem* **2016**, *9*, 547–561.
[36] A. Streitwieser, C. H. Heathcock, *Introduction to Organic Chemistry*, **1981**.
[37] T. Li, D. A. Harrington, *ChemSusChem* **2021**, *14*, 1472–1495.
[38] B. Liu, J. Greeley, *J. Phys. Chem. C* **2011**, *115*, 19702–19709.
[39] B. Liu, J. Greeley, *Phys. Chem. Chem. Phys.* **2013**, *15*, 6475–6485.
[40] D. Joubert, *Phys. Rev. B: Condens. Matter Mater. Phys.* **1999**, *59*, 1758–1775.
[41] J. P. Perdew, K. Burke, *Phys. Rev. B: Condens. Matter Mater. Phys.* **1996**, *54*, 16533–16539.
[42] S. Grimme, J. Antony, S. Ehrlich, H. Krieg, *J. Chem. Phys.* **2010**, *132*, 154104.
[43] S. Grimme, S. Ehrlich, L. Goerigk, *J. Comput. Chem.* **2011**, *32*, 1456–1465.
[44] S. Feng, J. Yi, H. Miura, N. Nakatani, M. Hada, T. Shishido, *ACS Catal.* **2020**, *10*, 6071–6083.
[45] J. K. Nørskov, F. Studt, F. Abild-Pedersen, T. Bligaard, Jens K. Nørskov, S. Felix, F. Abild-Pedersen, T. Bligaard, *Fundamental Concepts in Heterogeneous Catalysis*, John Wiley & Sons, Inc, Hoboken, NJ, USA.
[46] I. N. Levine, *Physical Chemistry*, McGraw-Hill Education, New York, NY, **2008**.
[47] Z. Wang, X. Liu, D. W. Rooney, P. Hu, *Surf. Sci.* **2015**, *640*, 181–189.

Manuscript received: February 10, 2023
Revised manuscript received: March 7, 2023
Accepted manuscript online: March 8, 2023
Version of record online: April 7, 2023